

Fig. 2

# Calculation

Since  $\lambda \gg R_0 \sqrt{\varepsilon}$

The field distribution is approximately quasi-static and can be calculated by the method of images.

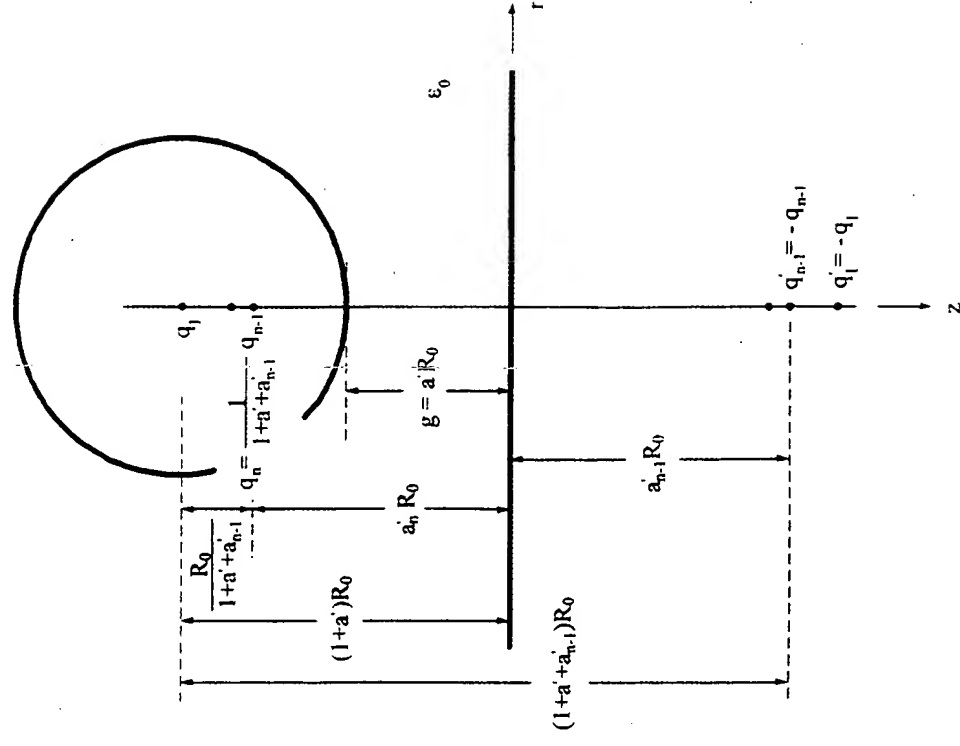


Fig. 3

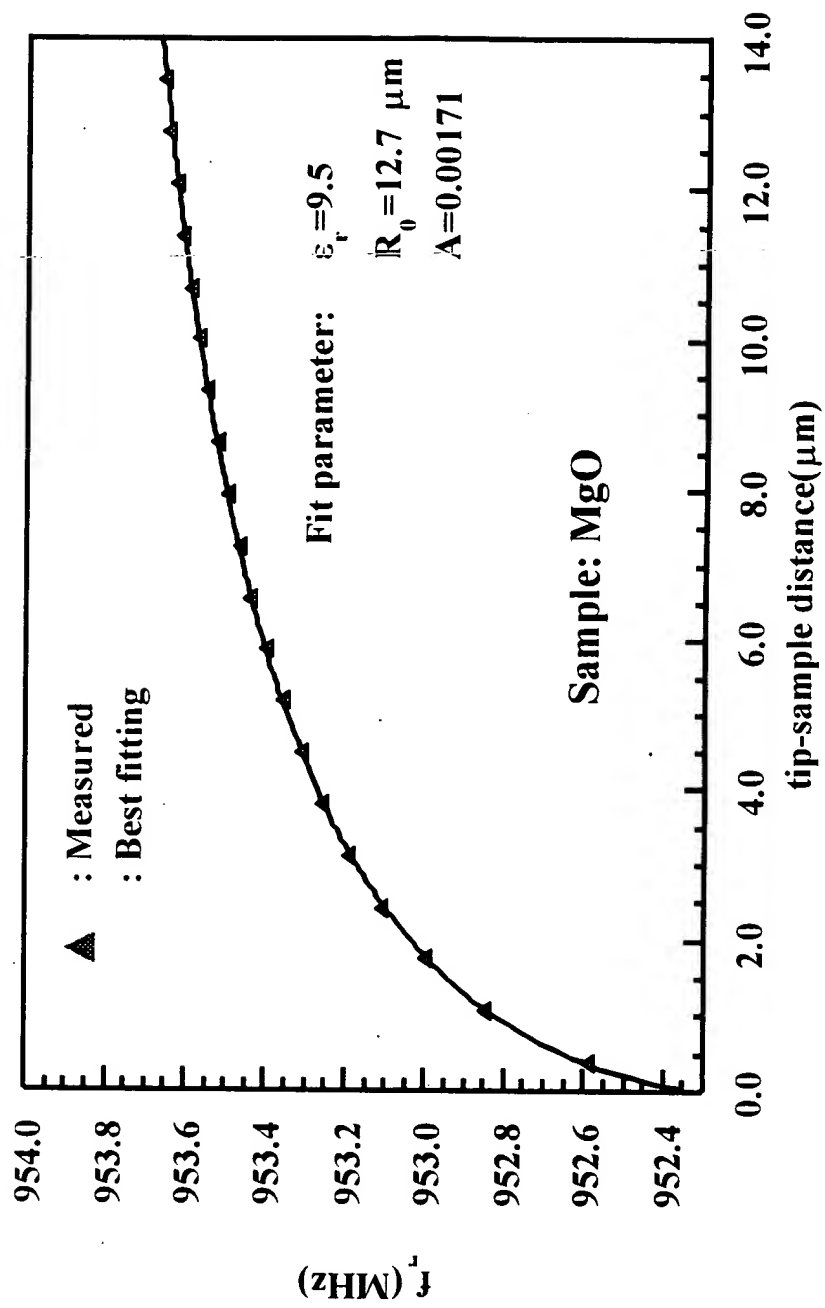
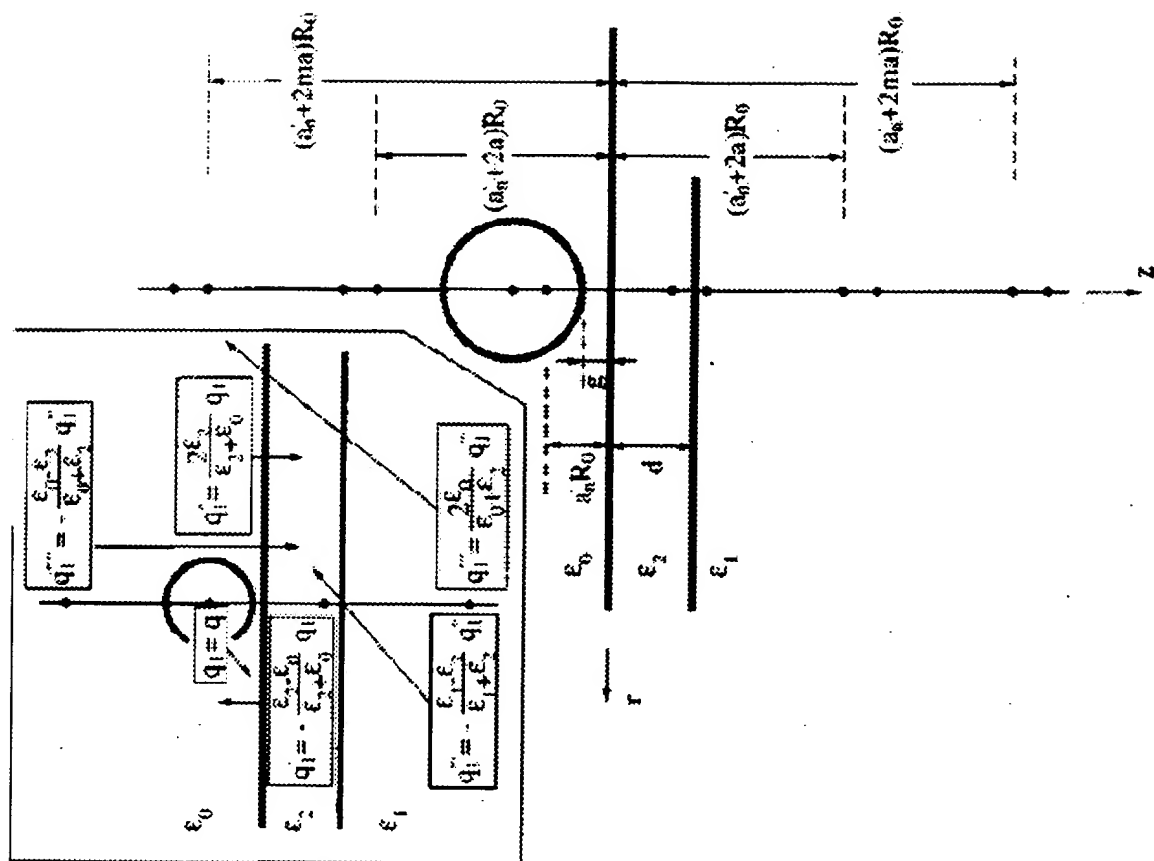


Fig. 4



$$\left(\frac{\delta f}{f_0}\right)\omega = A \epsilon_{333} E_1$$

$$\bar{E}_l = \frac{1}{32} \frac{V}{R_0} \frac{\epsilon_{33} + \epsilon_0}{2\epsilon_0}$$

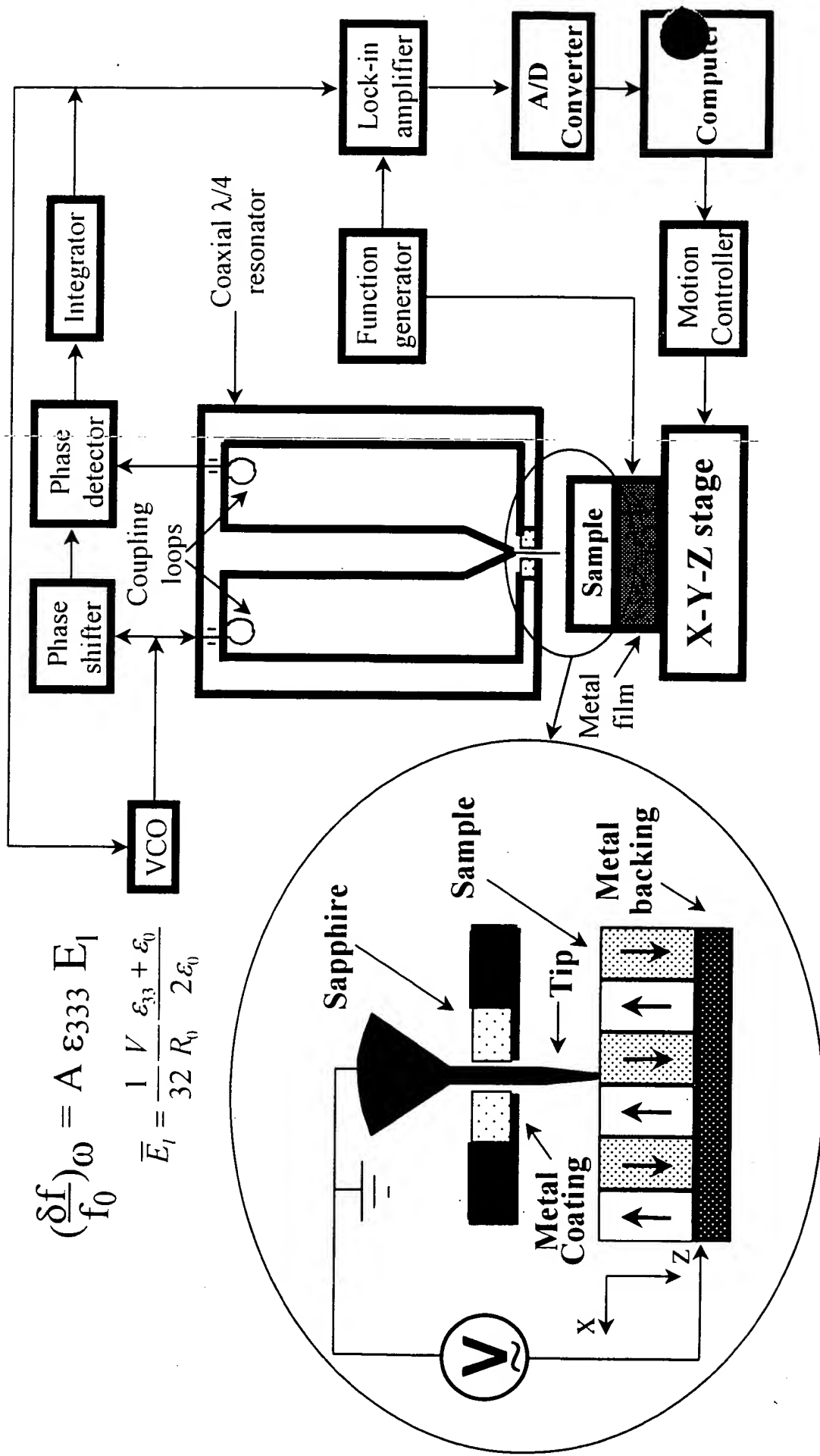
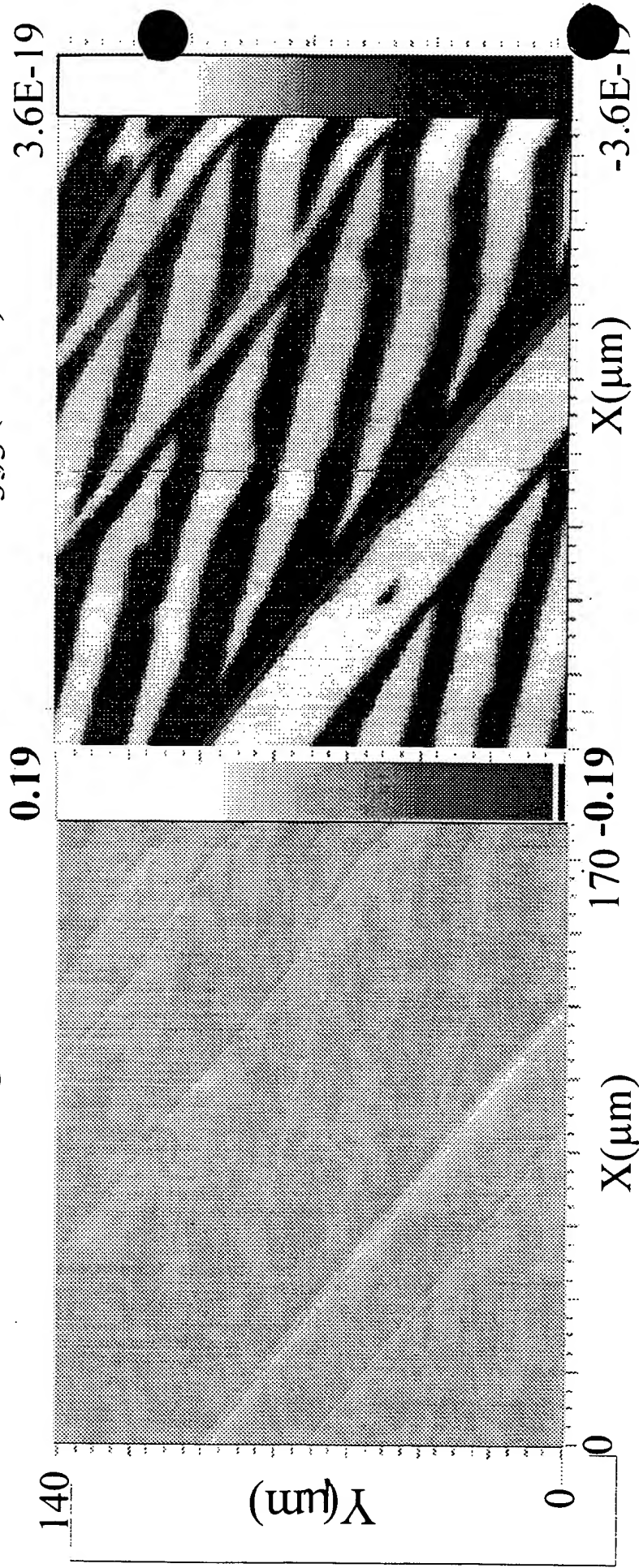


Fig. 6

$$\Delta \varepsilon_{33}(E_l) = \frac{\partial D_3}{\partial E_m} = \varepsilon_{33} + \varepsilon_{333}(E_l + E_m) + \frac{1}{2} \varepsilon_{3333}(E_l + E_m)^2 + \dots$$

$$\varepsilon_{333}(F/V)$$



*Sensitivity  $\Delta\varepsilon/\varepsilon \sim 10^{-3}$*

Fig. 7

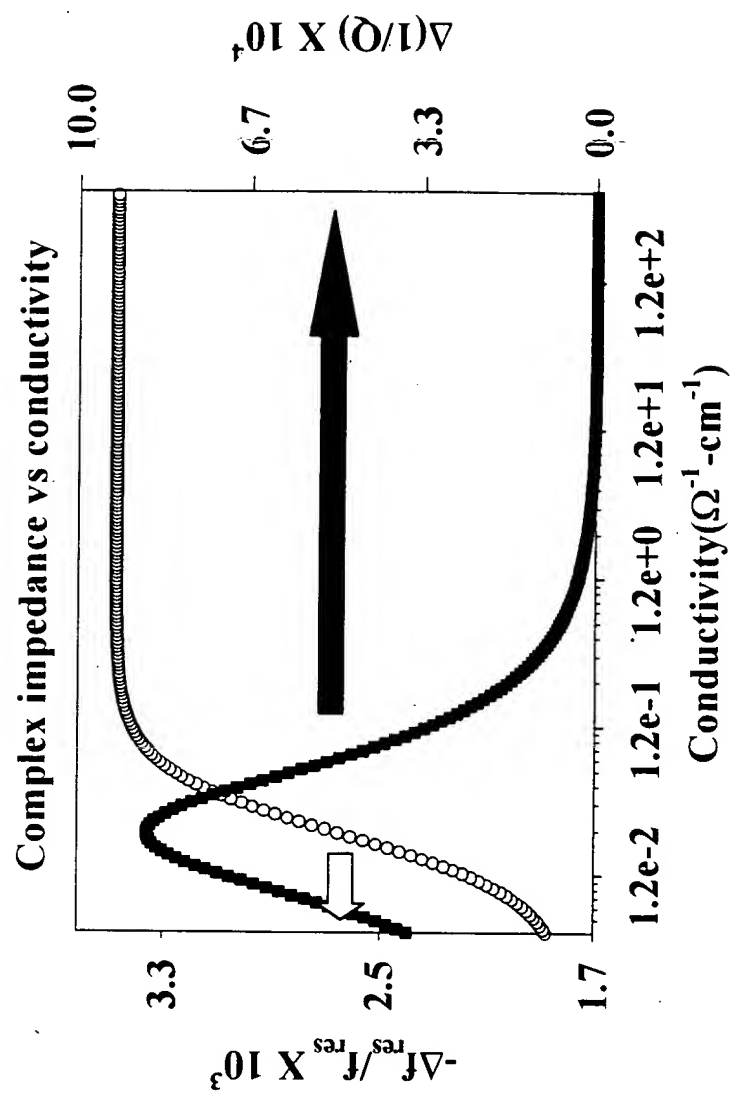


Fig. 8



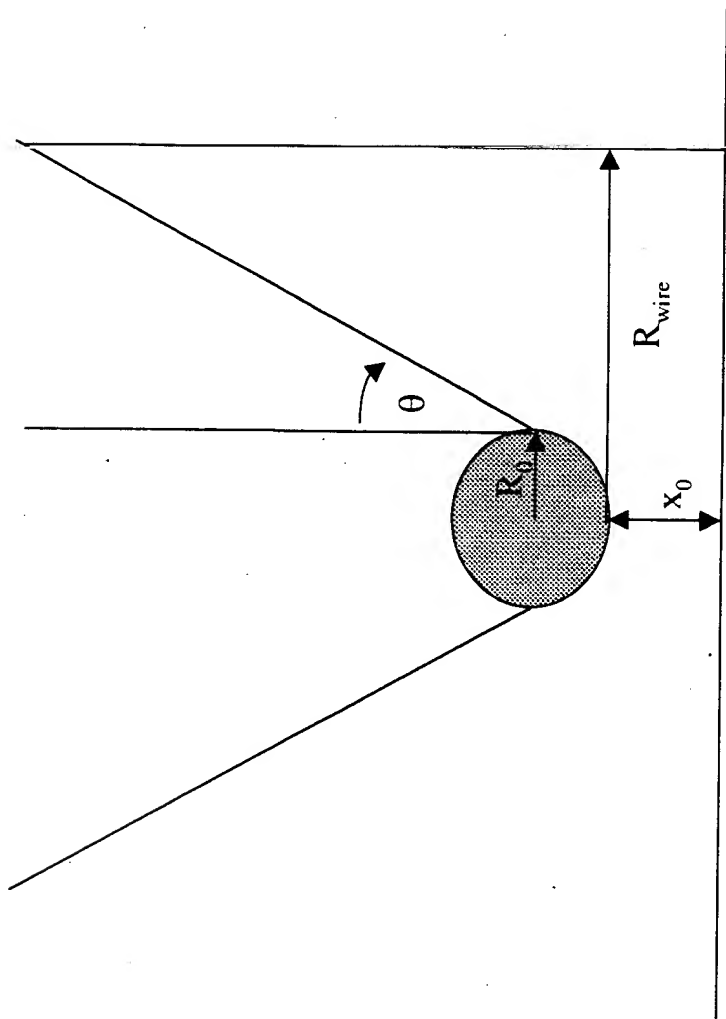
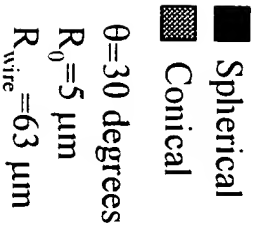


Fig. 9



1. The first part of the paper is devoted to the study of the properties of the function  $f(x)$  defined by the equation  $f(x) = \sum_{n=0}^{\infty} a_n x^n$ , where  $a_n$  are the coefficients of the power series.

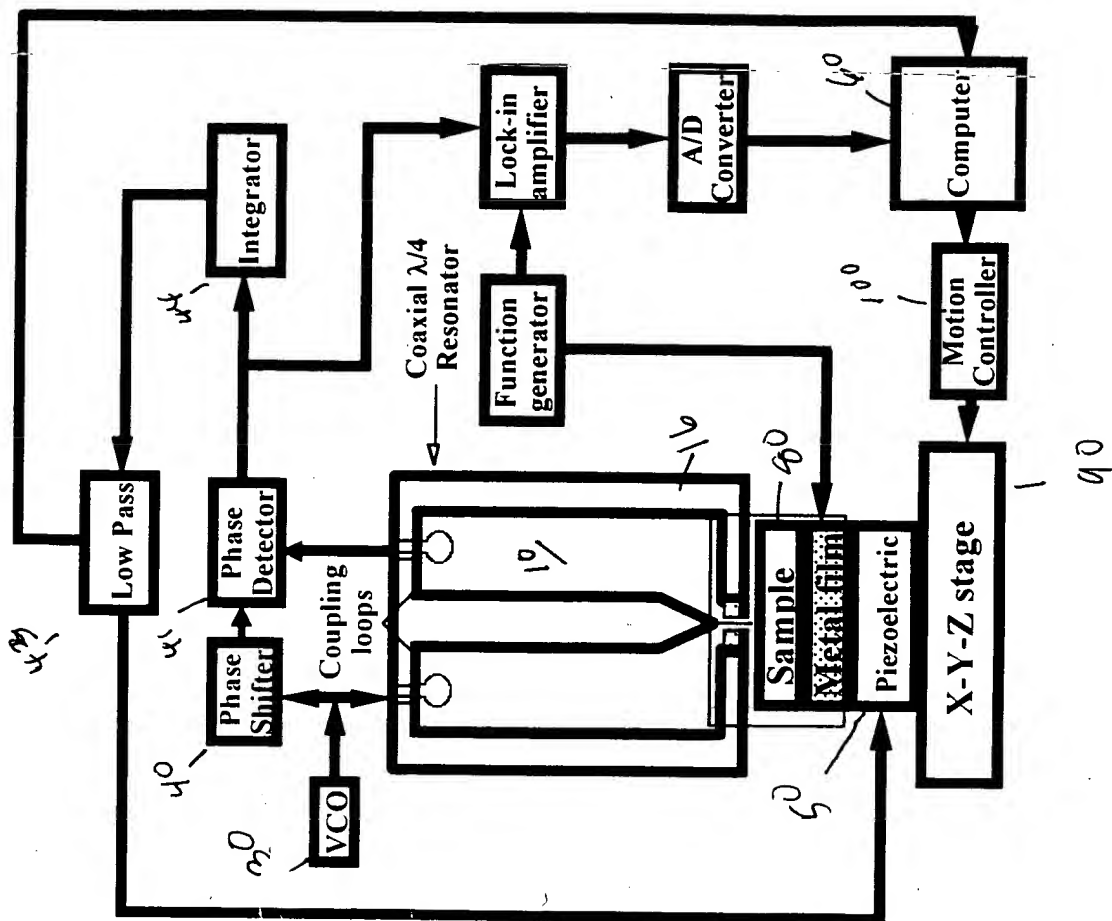


Figure 11

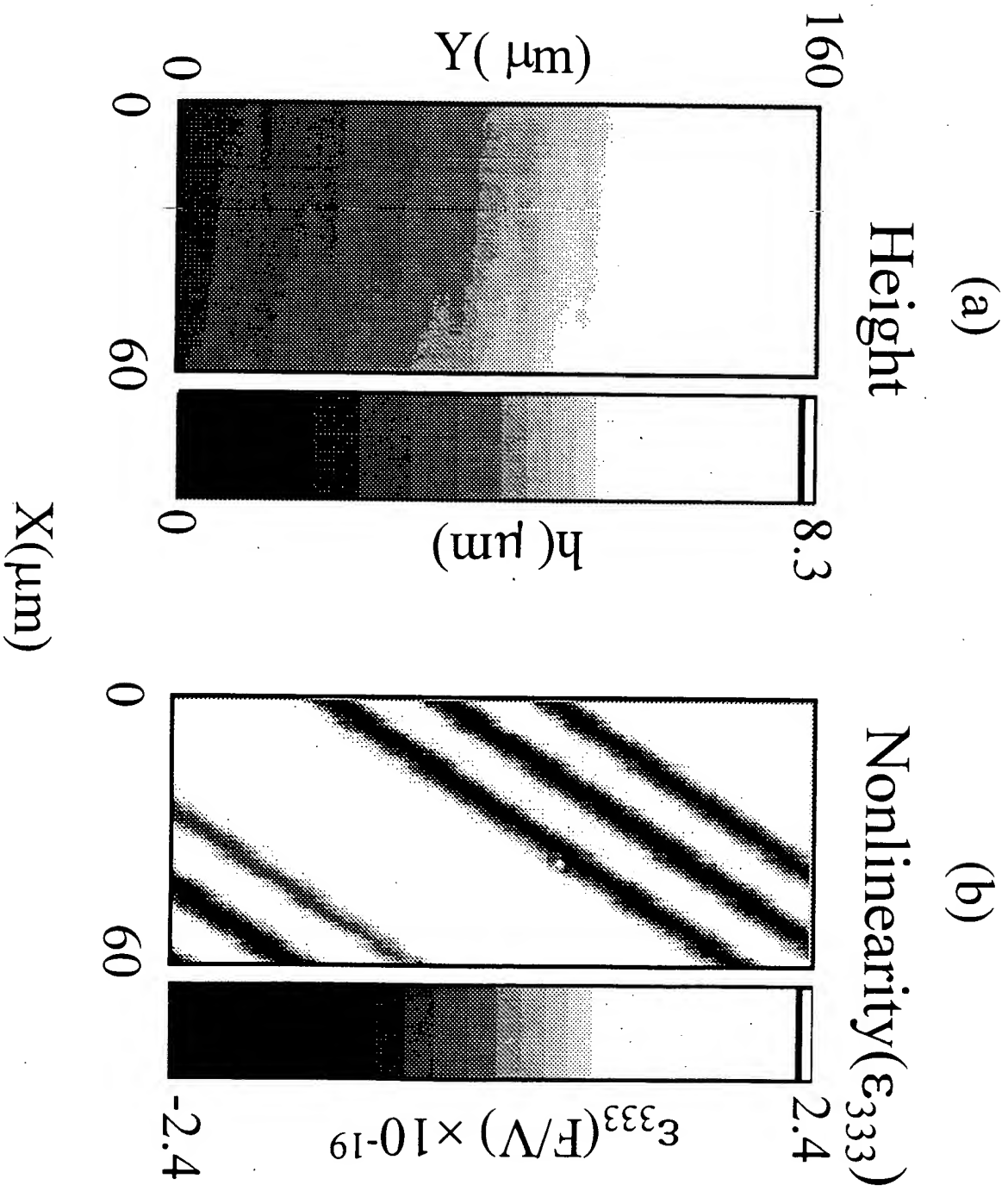


Figure 12

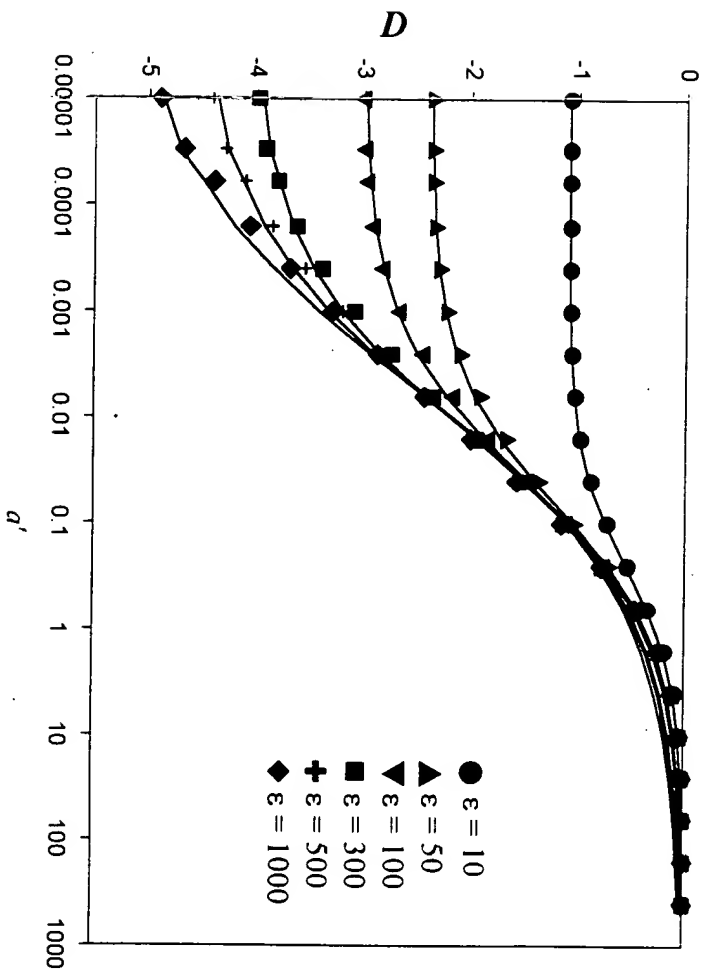


Fig. 13

1000 100 10 1 0.1 0.01 0.001 0.0001 0.00001

Derivative signal (pf/ $\mu\text{m}$ ) vs Tip-sample separation ( $\mu\text{m}$ )

Fig. 14 (a)

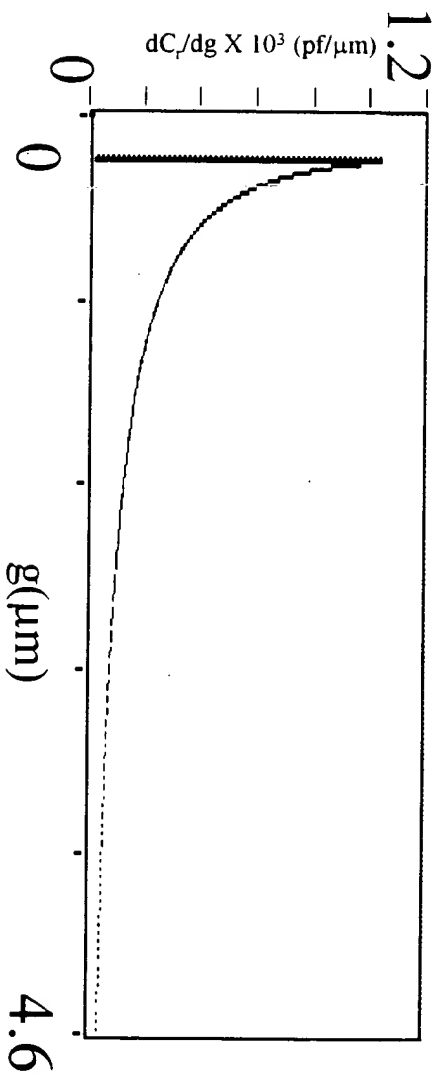


Fig. 14 (b)

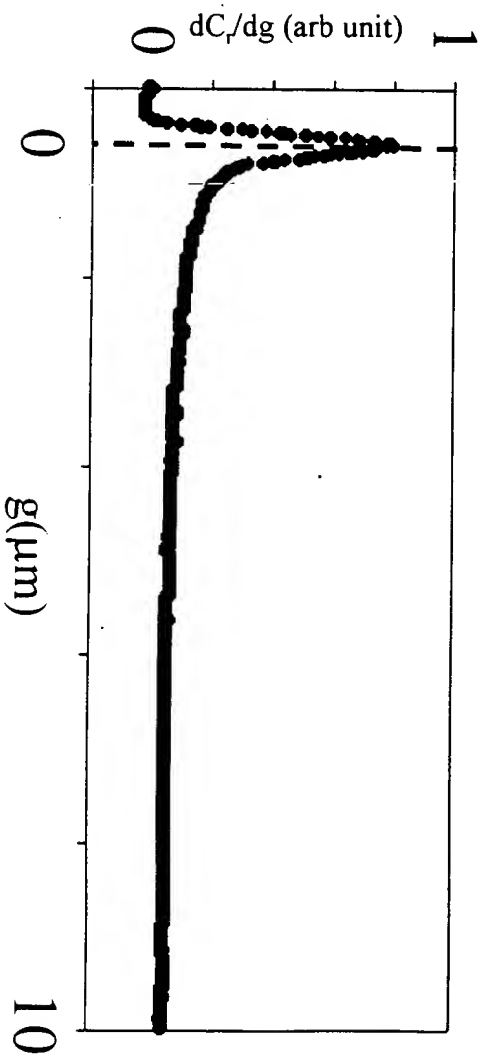


Fig. 14

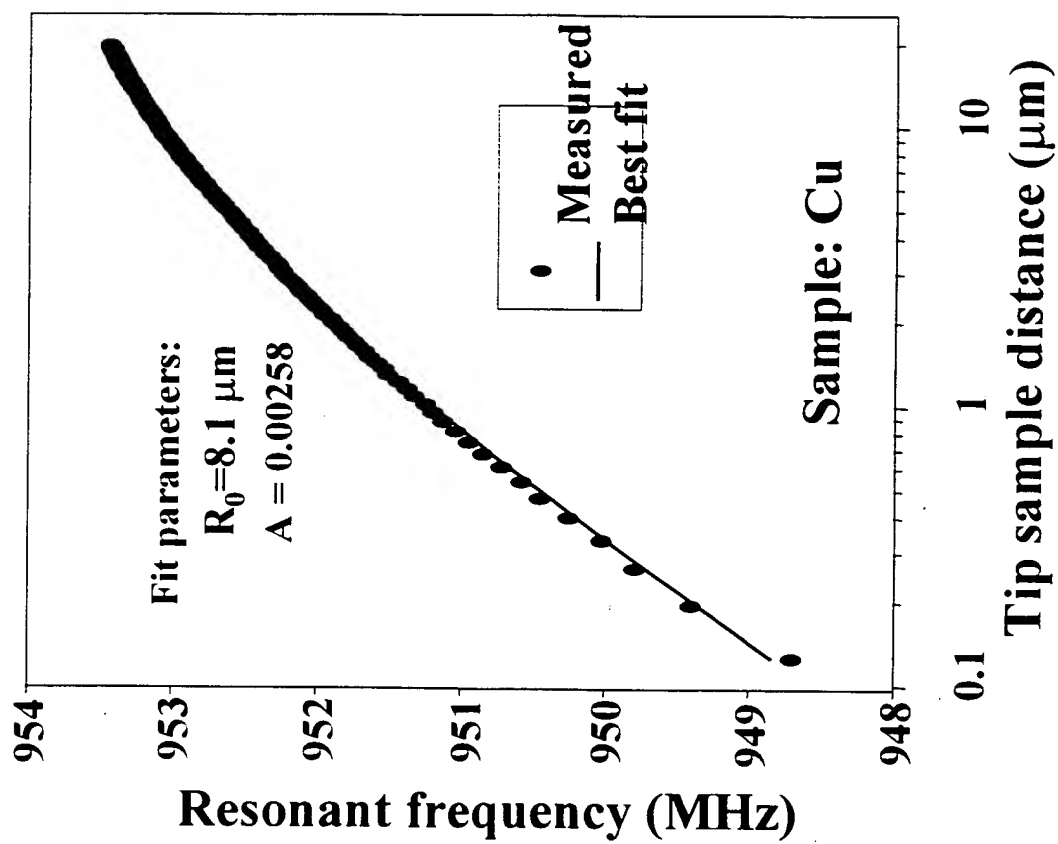
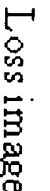
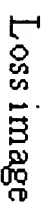


Fig. 15

Topographic image



Topographic image


$$\begin{array}{ccccccc} \{f^{(1)}_1\} & \{f^{(2)}_1\} & \{f^{(3)}_1\} & \{f^{(4)}_1\} & \{f^{(5)}_1\} & \{f^{(6)}_1\} & \{f^{(7)}_1\} \\ \{f^{(1)}_2\} & \{f^{(2)}_2\} & \{f^{(3)}_2\} & \{f^{(4)}_2\} & \{f^{(5)}_2\} & \{f^{(6)}_2\} & \{f^{(7)}_2\} \\ \vdots & \vdots & \vdots & \vdots & \vdots & \vdots & \vdots \\ \{f^{(1)}_n\} & \{f^{(2)}_n\} & \{f^{(3)}_n\} & \{f^{(4)}_n\} & \{f^{(5)}_n\} & \{f^{(6)}_n\} & \{f^{(7)}_n\} \end{array} \quad \begin{array}{c} \{f^{(1)}_1\} \\ \{f^{(2)}_1\} \\ \vdots \\ \{f^{(n)}_1\} \end{array} \quad \begin{array}{c} \{f^{(1)}_2\} \\ \{f^{(2)}_2\} \\ \vdots \\ \{f^{(n)}_2\} \end{array} \quad \begin{array}{c} \{f^{(1)}_3\} \\ \{f^{(2)}_3\} \\ \vdots \\ \{f^{(n)}_3\} \end{array} \quad \begin{array}{c} \{f^{(1)}_4\} \\ \{f^{(2)}_4\} \\ \vdots \\ \{f^{(n)}_4\} \end{array} \quad \begin{array}{c} \{f^{(1)}_5\} \\ \{f^{(2)}_5\} \\ \vdots \\ \{f^{(n)}_5\} \end{array} \quad \begin{array}{c} \{f^{(1)}_6\} \\ \{f^{(2)}_6\} \\ \vdots \\ \{f^{(n)}_6\} \end{array} \quad \begin{array}{c} \{f^{(1)}_7\} \\ \{f^{(2)}_7\} \\ \vdots \\ \{f^{(n)}_7\} \end{array}$$



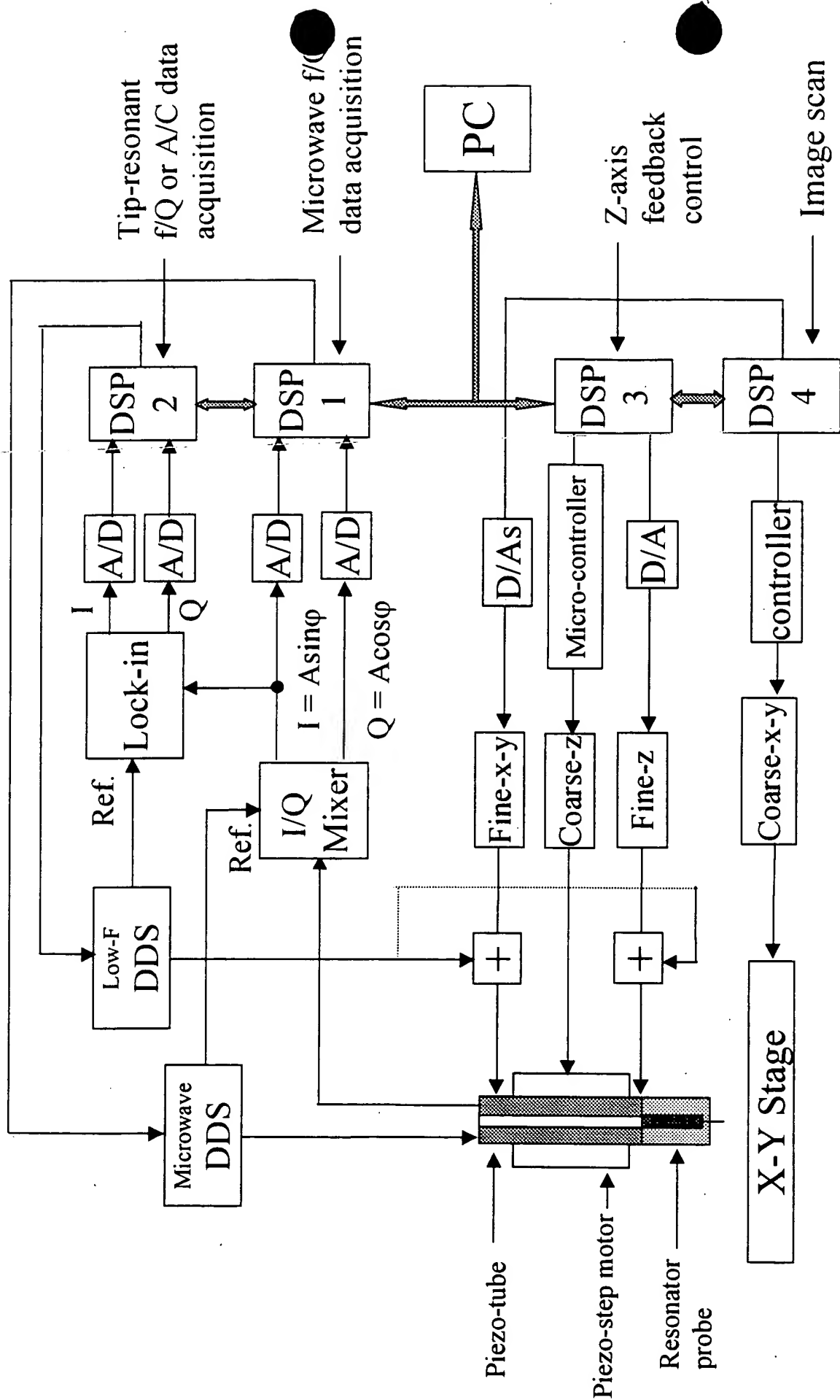


Fig. 17

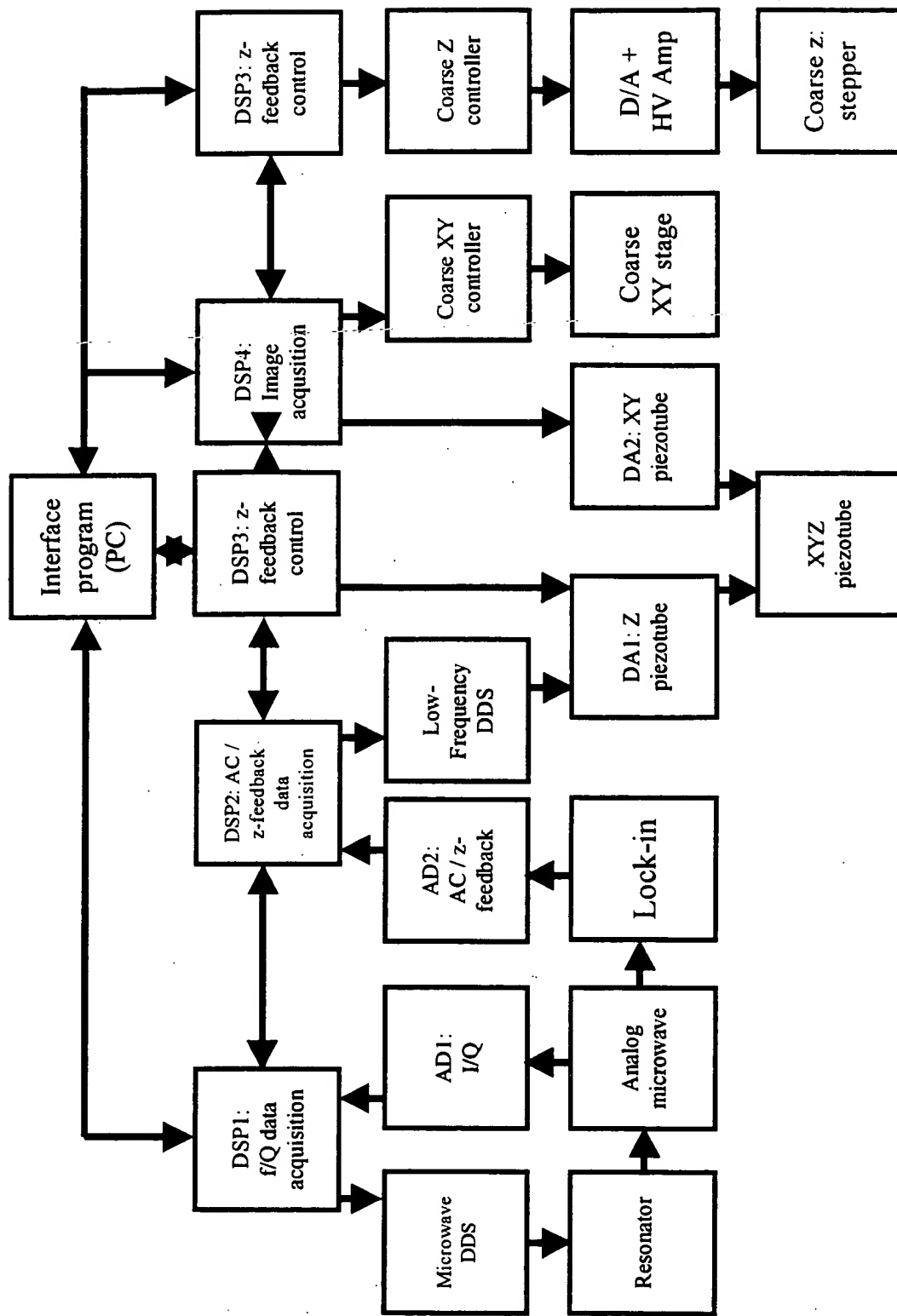


Fig. 18

Figure 19. Stepping mechanism. (a) Side view, (b) cross section view, (c) forward stepping, (d) backward stepping.

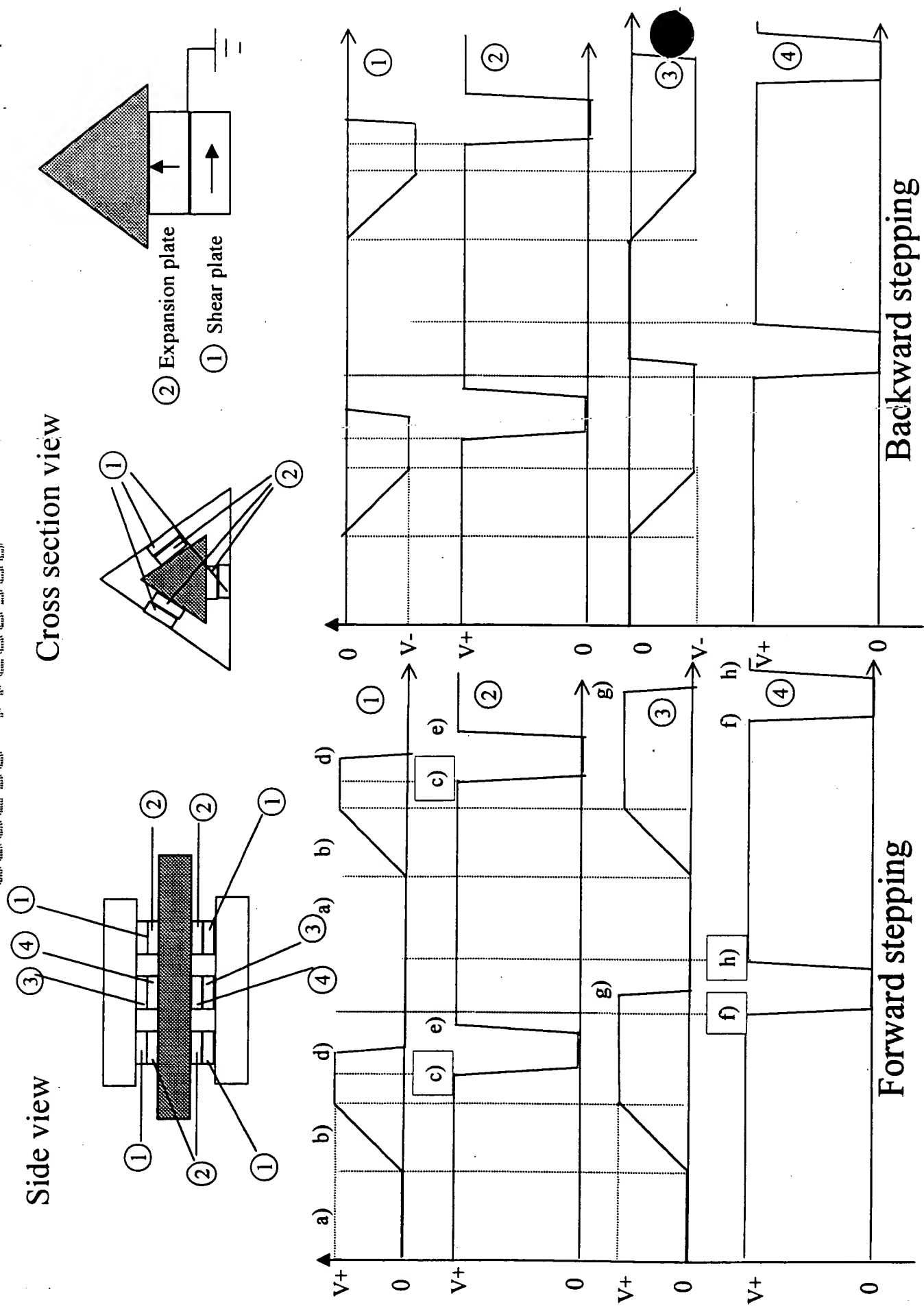
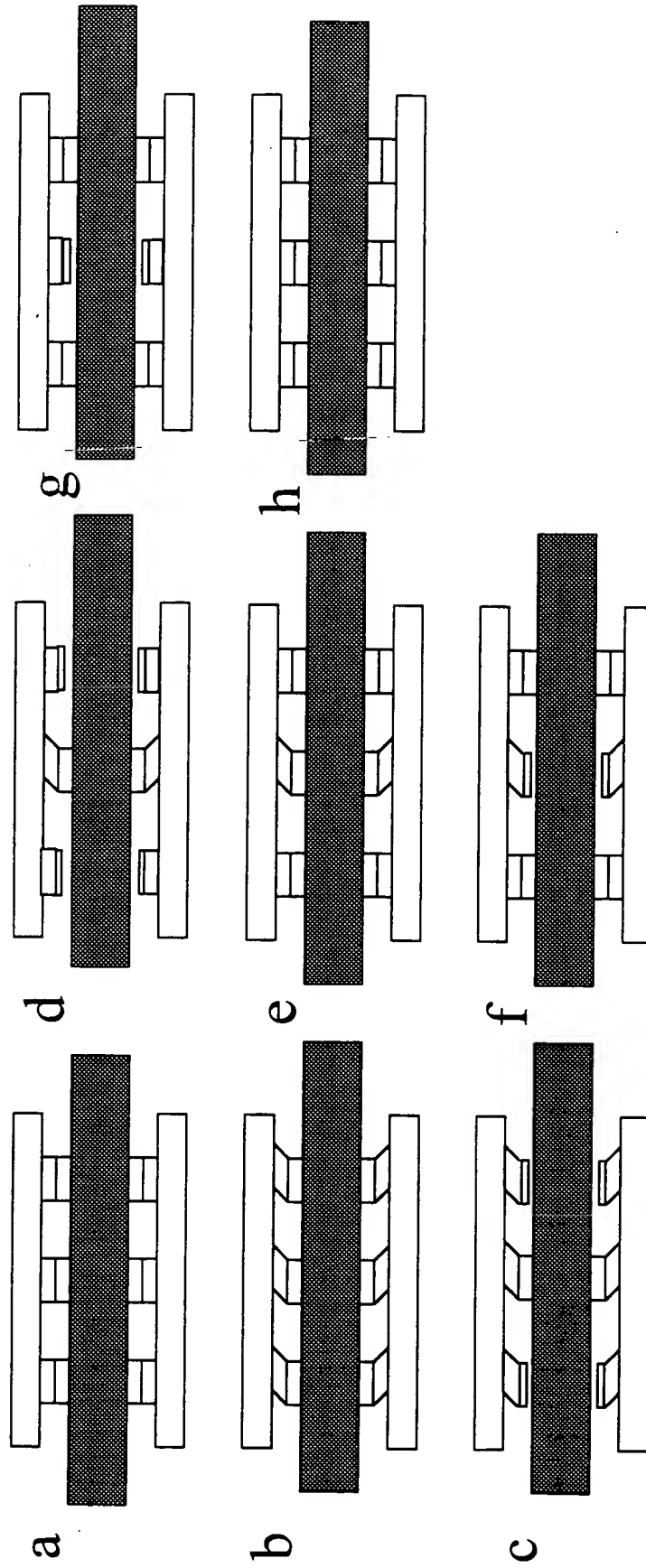


Figure 19.



## Integration of AFM

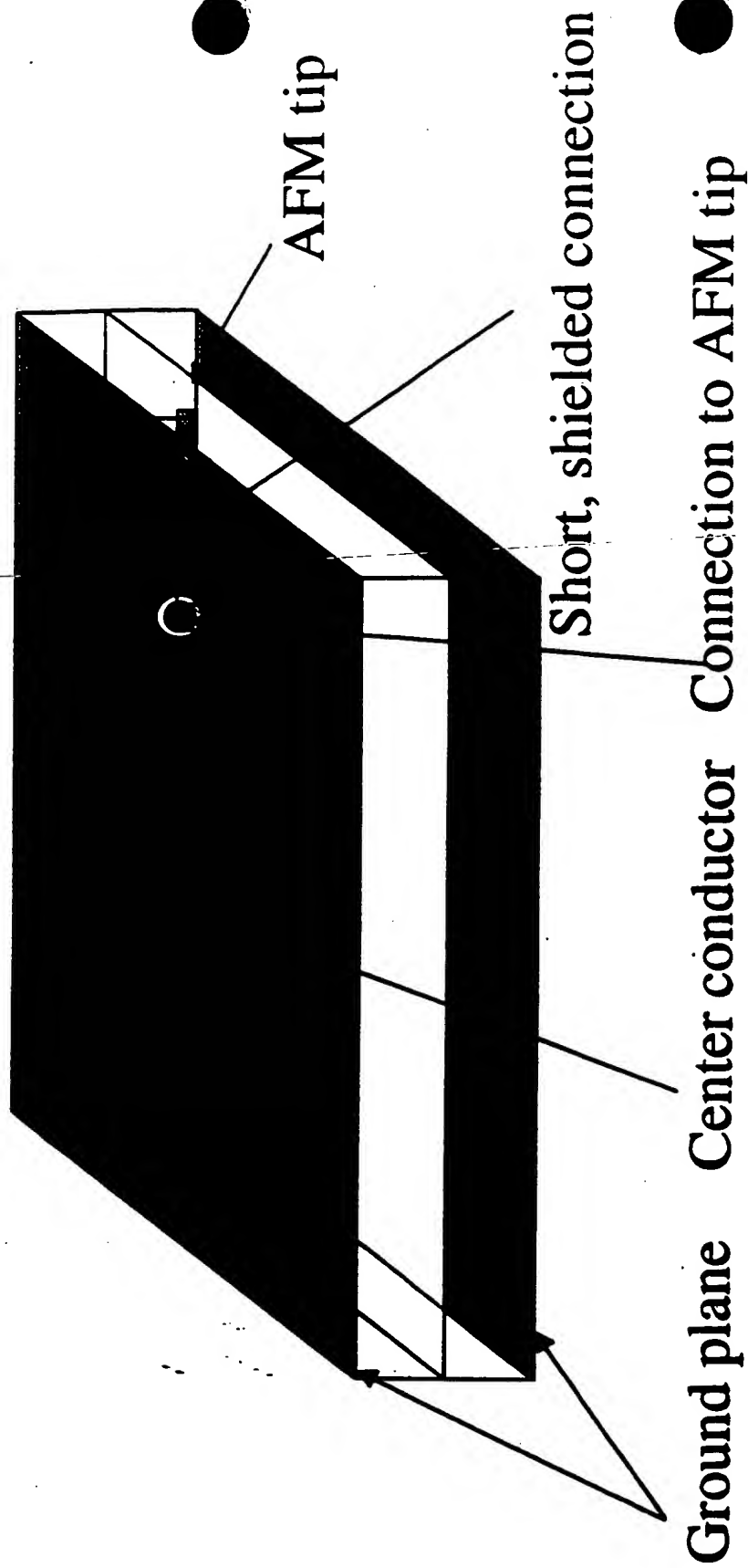


Figure 2/.

## Single Crystal Measurement

Material	Measured $\epsilon_r$	Reported $\epsilon_r$	Measured $\tan\delta$	Reported $\tan\delta$
YSZ	30.0	29	$1.7 \times 10^{-3}$	$1.75 \times 10^{-3}$
LaGaO <sub>3</sub>	23.2	25	$1.5 \times 10^{-3}$	$1.80 \times 10^{-3}$
CaNdAlO <sub>4</sub>	18.2	~19.5	$1.5 \times 10^{-3}$	$0.4 - 2.5 \times 10^{-3}$
TiO <sub>2</sub>	86.8	85	$3.9 \times 10^{-3}$	$4 \times 10^{-3}$
BaTiO <sub>3</sub>	295	300	0.47	0.47
YAlO <sub>3</sub>	16.8	16	-	$8.2 \times 10^{-5}$
SrLaAlO <sub>4</sub>	18.9	20	-	-
LaAlO <sub>3</sub>	25.7	24	-	$2.1 \times 10^{-5}$
MgO	9.5	9.8	-	$1.6 \times 10^{-5}$
LiNbO <sub>3</sub> (X-cut)	32.0	30	-	-

Table 1

Films	SEMM (1 GHz)		Interdigital Electrodes (1 GHz)	
	$\epsilon_r$	$\tan \delta$	$\epsilon_r$	$\tan \delta$
$\text{Ba}_{0.7}\text{Sr}_{0.3}\text{TiO}_3$	707	0.14	750	0.07
$\text{Ba}_{0.5}\text{Sr}_{0.5}\text{TiO}_3$	888	0.19	868	0.10
$\text{SrTiO}_3$	292	0.02	297	0.015
$\text{Ba}_{0.24}\text{Sr}_{0.35}\text{Ca}_{0.41}\text{TiO}_3$	150	0.05		
$\text{Ba}_{0.25}\text{Sr}_{0.35}\text{Ca}_{0.4}\text{TiO}_3$	240	0.05		

Table 2